

RESEARCH

Open Access



Metabolomics- and proteomics-based multi-omics integration reveals early metabolite alterations in sepsis-associated acute kidney injury

Pengfei Huang^{1,5†}, Yanqi Liu^{1,5†}, Yue Li^{3†}, Yu Xin^{1,5†}, Chuanchuan Nan^{1,2†}, Yinghao Luo^{1,5}, Yating Feng², Nana Jin², Yahui Peng^{1,5}, Dawei Wang^{4,5}, Yang Zhou^{1,5}, Feiyu Luan^{1,5}, Xinran Wang^{1,5}, Xibo Wang^{1,5}, Hongxu Li^{1,5}, Yuxin Zhou^{1,5}, Weiting Zhang^{1,5}, Yuhan Liu^{1,5}, Mengyao Yuan^{1,5}, Yuxin Zhang^{1,5}, Yuchen Song^{1,5}, Yu Xiao^{1,5}, Lifeng Shen^{1,5}, Kaijiang Yu^{1,5*}, Mingyan Zhao^{1,5*}, Lixin Cheng^{2*} and Changsong Wang^{1,5*}

Abstract

Background Sepsis-associated acute kidney injury (SA-AKI) is a frequent complication in patients with sepsis and is associated with high mortality. Therefore, early recognition of SA-AKI is essential for administering supportive treatment and preventing further damage. This study aimed to identify and validate metabolite biomarkers of SA-AKI to assist in early clinical diagnosis.

Methods Untargeted renal proteomic and metabolomic analyses were performed on the renal tissues of LPS-induced SA-AKI and sepsis mice. Glomerular filtration rate (GFR) monitoring technology was used to evaluate real-time renal function in mice. To elucidate the distinctive characteristics of SA-AKI, a multi-omics Spearman correlation network was constructed integrating core metabolites, proteins, and renal function. Subsequently, metabolomics analysis was used to explore the dynamic changes of core metabolites in the serum of SA-AKI mice at 0, 8, and 24 h. Finally, a clinical cohort (28 patients with SA-AKI vs. 28 patients with sepsis) serum quantitative metabolomic analysis was carried out to build a diagnostic model for SA-AKI via logistic regression (LR).

Results Thirteen differential renal metabolites and 112 differential renal proteins were identified through a multi-omics study of SA-AKI mice. Subsequently, a multi-omics correlation network was constructed to highlight five core metabolites, i.e., 3-hydroxybutyric acid, 3-hydroxymethylglutaric acid, creatine, myristic acid, and inosine, the early changes of which were then observed via serum time series experiments of SA-AKI mice. The levels

[†]Pengfei Huang, Yanqi Liu, Yue Li, Yu Xin and Chuanchuan Nan contributed equally to this work and are listed as co-first authors.

*Correspondence:

Kaijiang Yu
drkaijiang@163.com
Mingyan Zhao
mingyan1970@126.com
Lixin Cheng
easonlcheng@gmail.com
Changsong Wang
changsongwangicu@163.com

Full list of author information is available at the end of the article



of 3-hydroxybutyric acid, 3-hydroxymethylglutaric acid, and creatine increased significantly at 24 h, myristic acid increased at 8 h, while inosine decreased at 8 h. Ultimately, based on the identified core metabolites, we recruited 56 patients and constructed a diagnostic model named IC3, using inosine, creatine, and 3-hydroxybutyric acid, to early identify SA-AKI (AUC=0.90).

Conclusions We proposed a blood metabolite model consisting of inosine, creatine, and 3-hydroxybutyric acid for the early screening of SA-AKI. Future studies will observe the performance of these metabolites in other clinical populations to evaluate their diagnostic role.

Keywords Sepsis-associated acute kidney injury, Sepsis, Multi-omics analysis, Metabolome, Proteome, Diagnostic biomarkers

Background

Sepsis is a life-threatening organ dysfunction caused by a dysregulated immune response to infection. Deaths caused by sepsis account for approximately 20% of total global deaths [1, 2]. Approximately one-third of patients with sepsis in the intensive care unit (ICU) develop sepsis-associated acute kidney injury (SA-AKI) [3], and the mortality rate among patients with SA-AKI is as high as 41% [4]. AKI patients experience longer hospitalizations (+3.5 days) and higher medical costs (+\$9000) compared to those without renal impairment [5], emphasizing the critical need for early SA-AKI diagnosis.

Currently, the clinical diagnosis of AKI primarily relies on serum creatinine and urine output [6]. However, creatinine levels exhibit significant individual variability, while urine output is influenced by multiple factors such as fluid volume and cardiac function [7]. Moreover, studies have found that plasma neutrophil gelatinase-associated lipocalin (NGAL) is able to predict renal recovery in patients with SA-AKI [8], but the conclusion is not supported by other researches [9, 10]. For instance, Wong et al. discovered NGAL levels can increase in infectious patients without AKI [9]. Johan et al. found no difference in NGAL between patients with and without AKI [10]. Besides, kidney injury molecule-1 (Kim-1) is another biomarker for renal injury [11], but it is less studied in SA-AKI diagnosis. Thus, it is critical to explore new specific biomarkers for the early diagnosis of SA-AKI.

Renal metabolomics sequencing has focused on small molecular substances, identifying specific biomarkers for renal injury [12]. The integration of metabolomics with other high-throughput omics will be more conducive to the research on biomarkers [13, 14]. Moreover, a large number of machine learning algorithms have been developed and widely used to identify diagnostic and predictive biomarkers, such as support vector machine (SVM) and logistic regression [15–17]. For example, Luszczek et al. used machine learning methods to select three metabolites, lactic acid, 1-methylnicotinamide, and glycine, to predict the death of AKI patients [15]. This study employed proteomic and metabolomic techniques

to identify biomarkers associated with SA-AKI. The potential of core metabolites as early diagnostic biomarkers for SA-AKI was evaluated through time series of mice serum. Based on the above biomarkers, a diagnostic model for SA-AKI was constructed within a clinical cohort using machine learning techniques.

Methods

Study design

In this study, we aimed to identify biomarkers for early diagnosis of SA-AKI via multi-omics and clinical data (Fig. 1). Real-time fluorescence imaging technology was utilized to measure the glomerular filtration rate (GFR) [18, 19], combined with assessment of creatinine and blood urea nitrogen (BUN) to distinguish septic mice and SA-AKI mice. Then, we constructed an integrated Spearman correlation network for renal metabolomics and proteomics to highlight five core metabolites, i.e., 3-hydroxybutyric acid, 3-hydroxymethylglutaric acid, inosine, myristic acid, and creatine. The potential of these metabolites as early diagnostic biomarkers was then evaluated by tracking the changes in the activity of five core metabolites in mice serum at three distinct time points: 0, 8, and 24 h. Furthermore, three out of them (inosine, creatine, and 3-hydroxybutyric acid) were validated in a cohort including 56 patients (28 patients with SA-AKI vs. 28 patients with sepsis) using targeted quantitative metabolomics. Finally, we developed a logistic regression model to diagnose SA-AKI and to assess the severity of the disease.

SA-AKI mice construction

Twenty-eight male C57BL/6 mice (aged 8–10 weeks, weighing 25–30 g) were purchased from Charles River Laboratory Animal Technology Co. Ltd. (Beijing, China). The mice were placed in special cages with free access to food and water, four to each cage, and the cages were housed in a room with a 12-h light–dark cycle at a temperature of 22 °C.

Mice were randomly assigned to two parts. In the first part, sixteen mice received LPS (10 mg/kg, *i.p.*) and

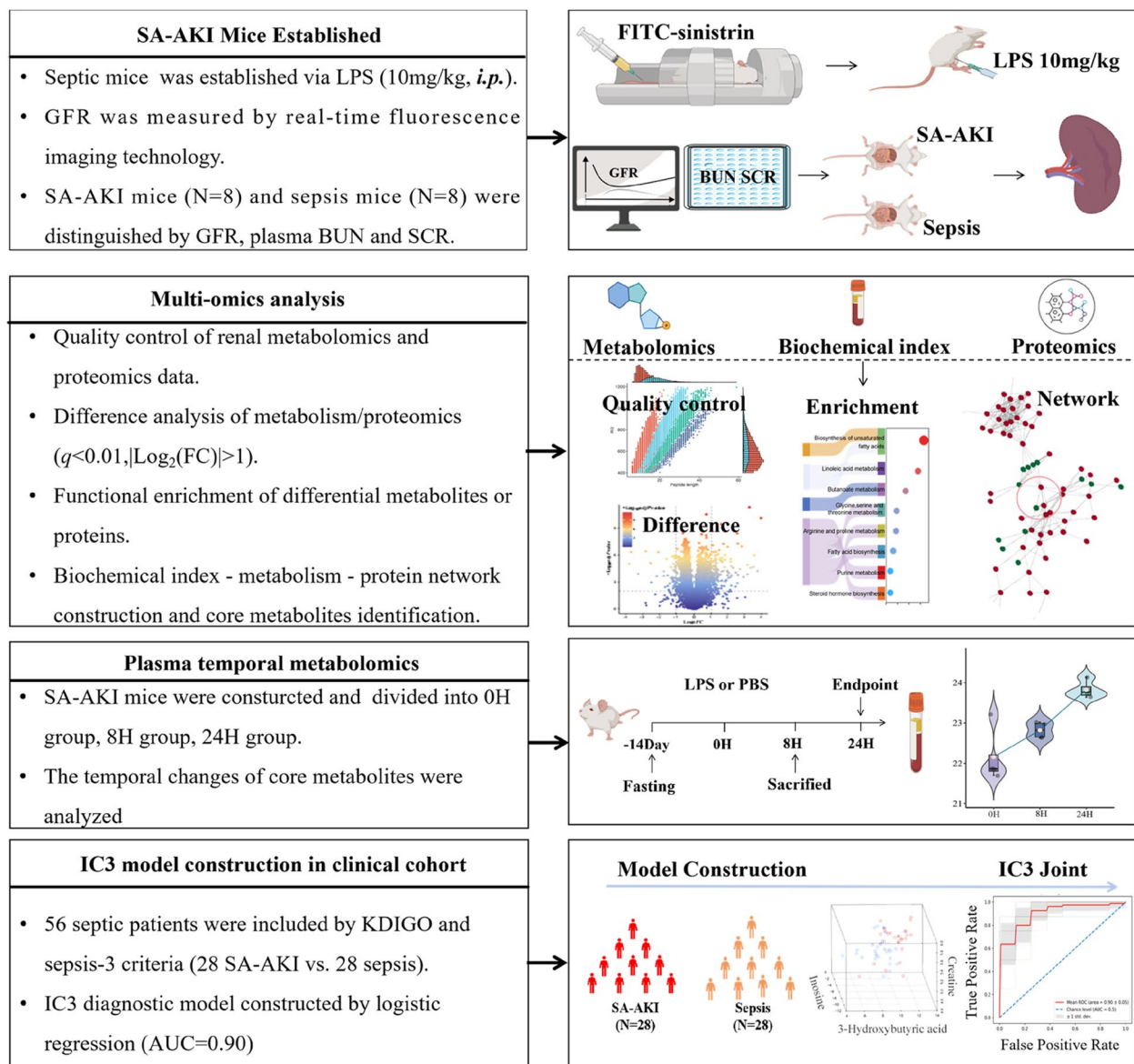


Fig. 1 Research design. Biotechnology, bioinformatics, and machine learning methods were integrated in this study to identify effective biomarkers for early diagnosis of SA-AKI. Firstly, SA-AKI and sepsis mice were established through LPS injection, with glomerular filtration rate measured via real-time fluorescence imaging. A Spearman correlation network was constructed from renal metabolomics, proteomics, and biochemical markers in SA-AKI and sepsis mice, from which five core metabolites were identified. Subsequently, we characterized the time series of core metabolites at 0, 8, and 24 h in septic mice to explore their potential as biomarkers for early diagnosis of SA-AKI. Finally, the IC3 model was established based on three core metabolites from a clinical cohort for early prediction of SA-AKI

were euthanized at 24 h. Septic mice or SA-AKI mice were differentiated by measuring glomerular filtration rate (GFR), blood urea nitrogen (BUN), and creatinine levels. In the second part, mice were divided into 3 groups for the experiment, with 4 mice in each group. They were killed at 8 and 24 h following the injection of LPS (10 mg/kg, *i.p.*). The 0-h group ($N=4$), serving as a control, received an intraperitoneal injection of an

equal volume of 0.9% saline. All animal experiments were conducted in compliance with National Institutes of Health guidelines and were approved by the Laboratory Animal Management and Welfare Ethics Committee of the First Affiliated Hospital of Harbin Medical University (Ethical Approval Number: 2023022). The detailed construction process of SA-AKI mice is described in the Additional file 1.

Patient recruitment and sample collection

From August 2022 to March 2023, a total of 56 patients (28 patients with SA-AKI vs. 28 patients with sepsis) were retrospectively enrolled for a clinical study at the Department of Critical Care Medicine, Second Affiliated Hospital of Harbin Medical University. Enrollment criteria included (1) aged between 18 and 65 years old, (2) patients with sepsis meeting the Sepsis-3 criteria [20], and (3) patients with SA-AKI meeting the Kidney Disease: Improving Global Outcomes (KDIGO) diagnostic criteria [21, 22], with an increase in serum creatinine of 0.3 mg/dl ($>26.5 \mu\text{mol/L}$) within 48 h, or an increase to more than 1.5 times the baseline value. Exclusion criteria were as follows: (1) discharge or death within 24 h after ICU admission, (2) presence of malignant tumors, (3) immunodeficiency or autoimmune diseases, and (4) insufficient clinical information. In accordance with standardized protocols, all pertinent clinical data were collected.

Peripheral venous blood samples were obtained from patients on the first day of diagnosis. The samples were centrifuged at 3000 rpm for 15 min, and 100 μl of supernatant serum from each sample was immediately frozen in liquid nitrogen and then stored at -80°C . The clinical investigation was approved by the Ethics Committee of the Second Affiliated Hospital of Harbin Medical University (Ethical Approval Number: KY2021-188) and strictly complied with the ethical standards of the Declaration of Helsinki.

Omics research

Detailed metabolomics, proteomic sequencing methods, and data quality control methods are presented in Additional file 1 [23–30].

Statistical analysis

Differential analysis

The values are expressed as mean \pm standard deviation (SD) (for continuous variables) or n (%) (for categorical variables). Difference analysis was performed using T -test (two-sided) on renal metabolomic (8 SA-AKI mice vs. 7 sepsis mice) and proteomic data (6 SA-AKI mice vs. 6 sepsis mice). The Benjamini–Hochberg correction was applied to control the false discovery rate (FDR), and the significant threshold was set to $q < 0.01$ and $|\text{Log}_2(\text{Fold Change})| > 1$. Time series serum metabolomics from SA-AKI mice (0 h–8 h–24 h, $N=4$) were performed via ANOVA test. Mice biochemical indicators (8 SA-AKI mice vs. 8 sepsis mice) and human serum targeted quantitative metabolomic sequencing data (28 patients with sepsis vs. 28 patients with SA-AKI) were measured by normality test, and then T -test (two-sided) or Wilcoxon sign-rank (two-sided) was decided. Serum-targeted

quantitative metabolomics sequencing data was then subgroup analyzed by sex, and the significance threshold was set at $p < 0.05$. Univariate logistic regression was applied to evaluate the impact of serum metabolites on SA-AKI, and the odds ratio (OR) was used as a quantitative index to describe the impact.

Correlation analysis and network construction

Spearman correlation analysis was used to explore the association between biochemical indicators and differential renal metabolites or proteins, and the significant threshold of the correlation was set at $q < 0.01$. Core metabolites with a metabolite-protein degree > 50 were identified. Multi-omics networks were constructed using Cytoscape (v3.10.0) software to elucidate their interactions and biological functions.

Machine learning models

Receiver operating characteristic (ROC) curves were generated to evaluate the diagnostic capability of 3-hydroxybutyric acid, creatine, and inosine in differentiating SA-AKI from patients with sepsis. Clinical cohort data were randomly divided into training (70%) and test (30%) sets. Four machine learning algorithms, including logistic regression (LR), random forest (RF), support vector machine (SVM), and extreme gradient boosting (XGB), were applied to train diagnostic models. Model performance was robustly estimated by calculating the average AUC across 10 independent test sets. Statistical analysis and modeling procedures were performed via RStudio (v4.2.2).

Results

Metabolomic variations between SA-AKI and sepsis

Plasma BUN (65 [46,76] vs. 8.19 [7.28,9.1], $p < 0.05$) and creatinine (70 [62,73] vs. 28 [26,30], $p < 0.05$) were significantly higher in SA-AKI mice than in sepsis mice, and GFR (0.59 ± 0.08 vs. 0.95 ± 0.17 , $p < 0.05$) was significantly lower in SA-AKI mice than in sepsis mice ($p < 0.05$) (Fig. 2a; Additional file 2: Table S1). Combining with GFR, BUN, and creatinine indicated that the SA-AKI mice were successfully established [23].

There was a clear change in metabolic activity between SA-AKI mice and sepsis mice (Fig. 2b). The thirteen renal metabolites with significant changes between SA-AKI and sepsis were detailed in Table 1, among which eleven are upregulated and two are downregulated ($q < 0.01$, $|\text{Log}_2(\text{FC})| > 1$) (Fig. 2d–e; Additional file 2: Table S2–3). The differential metabolites primarily participate in pathways such as biosynthesis of unsaturated fatty acids, linoleic acid metabolism, and butanoate metabolism (Fig. 2f). Among them, linoleic acid is a product of linoleic acid

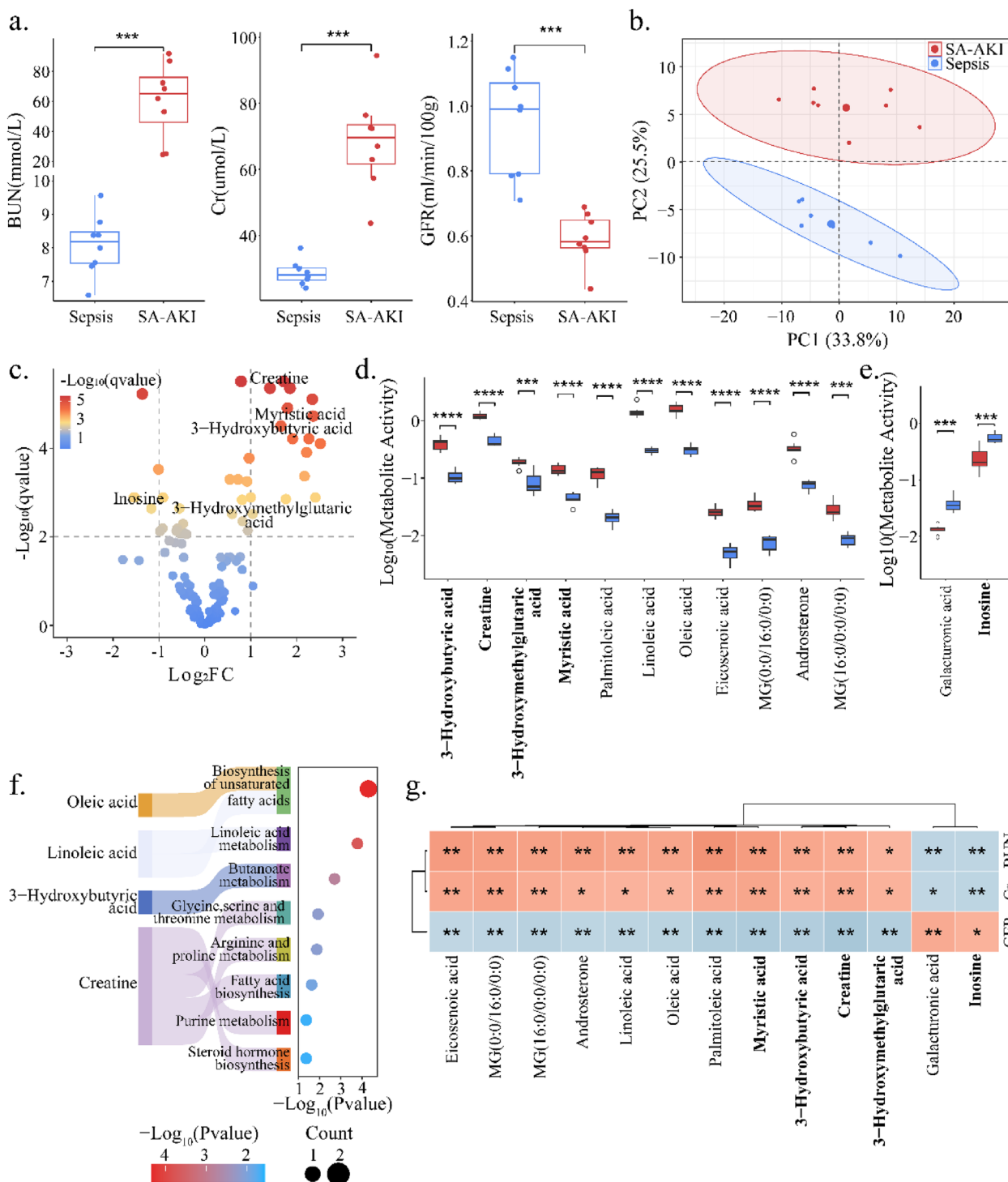


Fig. 2 Systematic analysis of metabolic activity differences between SA-AKI and sepsis. **a** Box plots present the biochemical indicators in SA-AKI and sepsis mice, including BUN, creatinine, and GFR. **b** PCA plot of renal metabolomics. Blue points represent the sepsis group ($N=7$), while red points represent the SA-AKI group ($N=8$). **c** Differential analysis of renal metabolomics between the two groups. Colors of points correspond to q -values. Significant after Benjamini–Hochberg adjusted two-tailed t -test ($q < 0.01$) and $|\text{Log}_2(\text{Fold Change})| > 1$. **d** Activity distribution of the 11 upregulated metabolites. **e** Activity distribution of the 2 downregulated metabolites. Red represents the SA-AKI group and blue represents the sepsis group. **f** Kegg pathway analysis on renal differential metabolites. **g** Heatmap illustrating the Spearman correlation coefficients between the 13 differential metabolites and the three biochemical indicators. Orange represents a positive correlation and light blue represents a negative correlation. *, **, and *** indicate $q < 0.05$, $q < 0.01$, and $q < 0.001$, respectively

Table 1 Differentially regulated metabolites between SA-AKI and sepsis group

Name	HMDB IDs	Log ₂ FC	q-values
Palmitoleic acid	HMDB0003229	2.52	< 1e−04
Eicosenoic acid	HMDB0002231	2.36	< 1e−04
Oleic acid	HMDB0000207	2.34	< 1e−05
Linoleic acid	HMDB0000673	2.27	< 1e−04
MG(0:0/16:0/0:0)	HMDB0011533	2.22	< 1e−03
Androsterone	HMDB0000031	2.17	< 1e−03
3-Hydroxybutyric acid	HMDB0000011	1.91	< 1e−04
MG(16:0/0:0/0:0)	HMDB0011564	1.76	< 1e−02
Myristic acid	HMDB0000806	1.66	< 1e−04
Creatine	HMDB0000064	1.42	< 1e−05
3-Hydroxymethylglutaric acid	HMDB0000355	1.04	< 1e−02
Inosine	HMDB0000195	−1.17	< 1e−02
Galacturonic acid	HMDB0002545	−1.53	< 1e−02

metabolism. Zeng et al. has found that reducing linoleic acid can ameliorate cisplatin-induced AKI [31]. In addition, studies have indicated that linoleic acid breakdown products are associated with acute respiratory distress syndrome and sepsis-related deaths in severe COVID-19 patients [32, 33]. Notably, each differential metabolite was significantly correlated with at least one renal function indicator ($q < 0.01$) (Fig. 2g), suggesting a potential link between changes in renal metabolism and renal impairment.

Specifically, 3-hydroxybutyric acid ($\text{Log}_2(\text{FC}) = 1.91$) and creatine ($\text{Log}_2(\text{FC}) = 1.42$) were significantly increased, while inosine was significantly decreased in SA-AKI mice ($\text{Log}_2(\text{FC}) = -1.17$). In addition, both of 3-hydroxybutyric acid and creatine were negatively correlated with GFR ($R = -0.80$, $R = -0.90$) while these two metabolites were positively associated with BUN ($R = 0.73$, $R = 0.69$). Inosine was negatively correlated with BUN ($R = -0.67$). These results highlighted the important effects of these metabolites in SA-AKI mice and revealed potential mechanisms of renal injury.

Proteomic and metabolomic network analysis identifies core metabolites

The protein expression significantly changed between SA-AKI mice and sepsis mice (Fig. 3a). Renal proteins significantly dysregulated in SA-AKI mice compared with sepsis ($q < 0.01$, $|\text{Log}_2(\text{FC})| > 1$), with 122 being up-regulated and 42 down-regulated (Fig. 3b; Additional file 3: Table S1). 112 differential proteins associated with renal function were detected for further analysis ($q < 0.01$) (Additional file 3: Fig. S1b).

KEGG pathway analysis showed that renal differential proteins were mainly involved in inflammatory pathways such as NF-kappa B signaling pathway, IL-17 signaling pathway, and Toll-like receptor signaling pathway. Activation of cell death pathways such as adipocytokine signaling pathway, ferroptosis, and apoptosis pathway were also found (Fig. 2c). These may be related to the impaired mitochondrial function during the occurrence of SA-AKI [14, 34]. Gene enrichment analysis found that biological process (BP) was mainly enriched in reactive oxygen species biosynthetic process, iron ion transmembrane transport, macrophage activation, and regulation of lipid metabolic process (Additional file 3: Fig. S1c), cell composition (CC) was enriched in lipoprotein particle, high-density lipoprotein particle, lipid droplet (Additional file 3: Fig. S1d), molecular functional (MF) process was enriched in oxidoreductase activity, acting on metal ions and lipid transporter activity (Additional file 3: Fig. S1e). Abnormal lipid metabolism can trigger an inflammatory response that promotes cell death [35], leading to a poor prognosis for AKI [36].

Renal metabolomic and proteomic expressions were strongly correlated, for instance, consistent change was found between 3-hydroxybutyric acid and Mphosph10 in our research ($\text{cor} > 0.99$, $q < 0.01$) (Fig. 3c). 3-Hydroxymethylglutaric acid, 3-hydroxybutyric acid, creatine, myristic acid, and inosine were considered as core metabolites of SA-AKI, with a metabolite-protein connectivity threshold of 50 (Fig. 3d). Significant associations ($q < 0.01$) were found between 32 proteins, 5 core metabolites, and renal function indicators, highlighting the continuous interaction between multi-omics within the SA-AKI renal system (Fig. 3e). The 28 upregulated and 4

(See figure on next page.)

Fig. 3 Integrated analysis of mice renal metabolomic and proteomic data. **a** PCA plot of renal proteomics. Blue points represent the sepsis group ($N = 6$), while red points represent the SA-AKI group ($N = 6$). **b** Differential analysis of renal proteomics between the two groups. Colors of points correspond to q -values. Significant after Benjamini–Hochberg adjusted two-tailed t -test ($q < 0.01$) and $|\text{Log}_2(\text{Fold Change})| > 1$. **c** KEGG pathway analysis on renal differential proteins. **d** Spearman correlation between differential renal proteins and 16 differential renal metabolites. Orange represents a positive correlation while light blue represents a negative correlation. **e** Degree distribution for the differential metabolites, among which metabolite-protein degree > 50 were defined as core metabolites. **f** Sankey diagram depicting the interrelationships between renal proteins, core renal metabolites, and biochemical indicators. Red lines represent positive correlation, and light blue lines represent negative correlation. Red grid indicates up-regulation and light blue grid indicates down-regulation in SA-AKI mice. **g** Differential proteins related to the five core metabolites

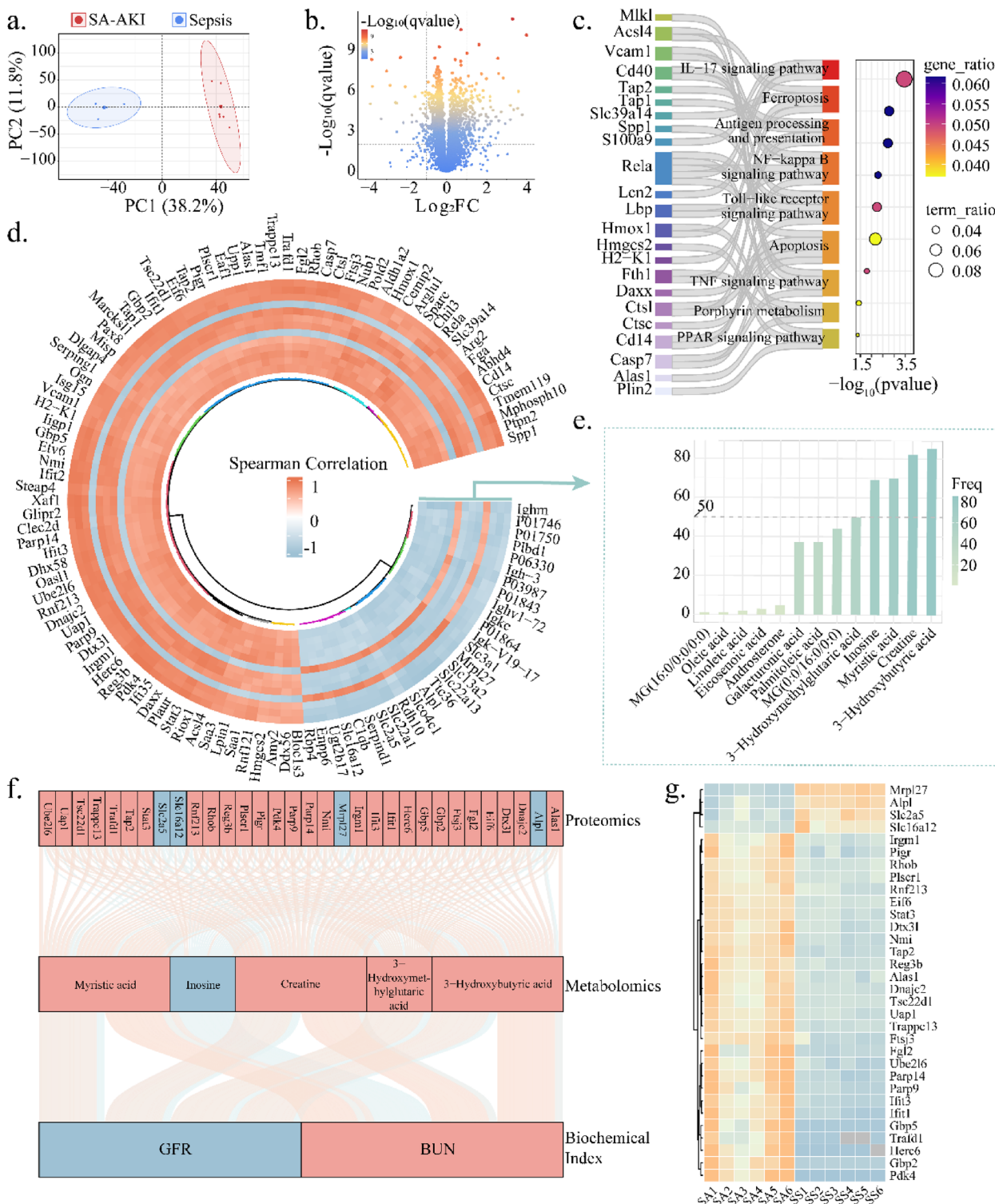


Fig. 3 (See legend on previous page.)

downregulated proteins may be linked to the function of core metabolites, implicated in the regulation of immune response (Fig. 3f–g; Additional file 3: Fig. S1c–e).

Five core metabolites, along with 112 differential renal proteins and 13 differential renal metabolites, were involved in regulating changes in renal function through

network analysis (Fig. 4). Core metabolites may play a crucial role in the progression of sepsis to SA-AKI, which may provide potential strategies for clinical diagnosis.

Serum time series investigation of core metabolites in SA-AKI mice

We performed serum metabolomic analyses of SA-AKI mice at three time points (0 h, 8 h, 24 h) to investigate the triggering time of the core metabolites (Fig. 5a;

Additional file 4: Table S1). The metabolic activities of 3-hydroxymethylglutaric acid, creatine, and 3-hydroxymethylglutaric acid changed significantly from 0 to 8 h to 24 h ($p < 0.05$, ANOVA test), while inosine and myristic acid remained stable ($p > 0.05$, ANOVA test). Specifically, the metabolic activity of 3-hydroxymethylglutaric acid, 3-hydroxybutyric acid, and creatine significantly increased from 0 to 24 h and from 8 to 24 h ($p < 0.05$) (Fig. 5b–d). Inosine showed a descent trend from 0

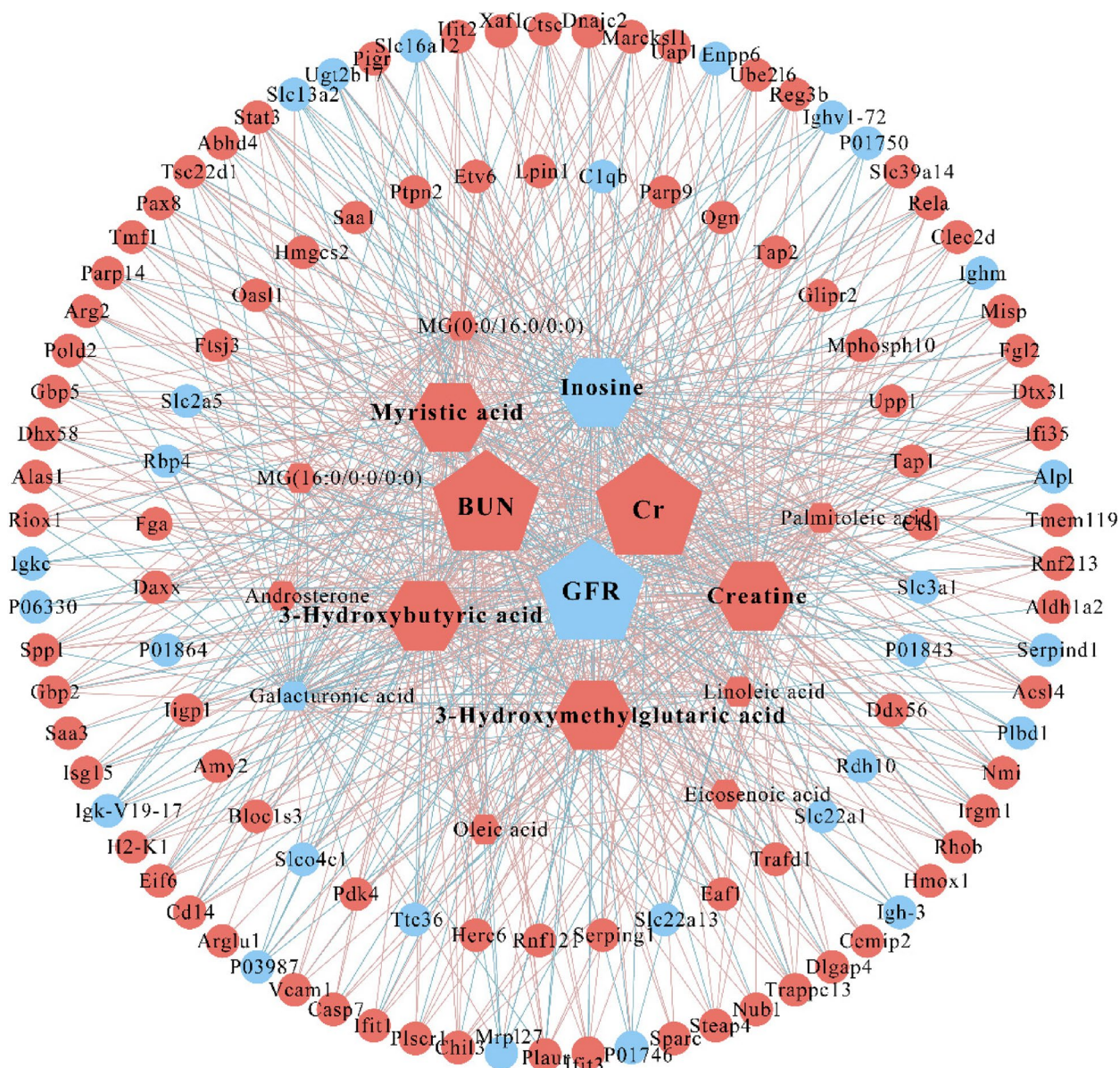


Fig. 4 Multi-omics network of SA-AKI. Proteins and metabolites correlated to the core metabolites and biochemical indicators are shown in the network. Biochemical indicators, core metabolites, and renal proteins are represented by pentagon, hexagon, and circle, respectively. Red vertex indicates up-regulation and blue vertex indicates down-regulation between SA-AKI and sepsis groups. Red edge represents a positive correlation and blue edge represents a negative correlation between the vertices

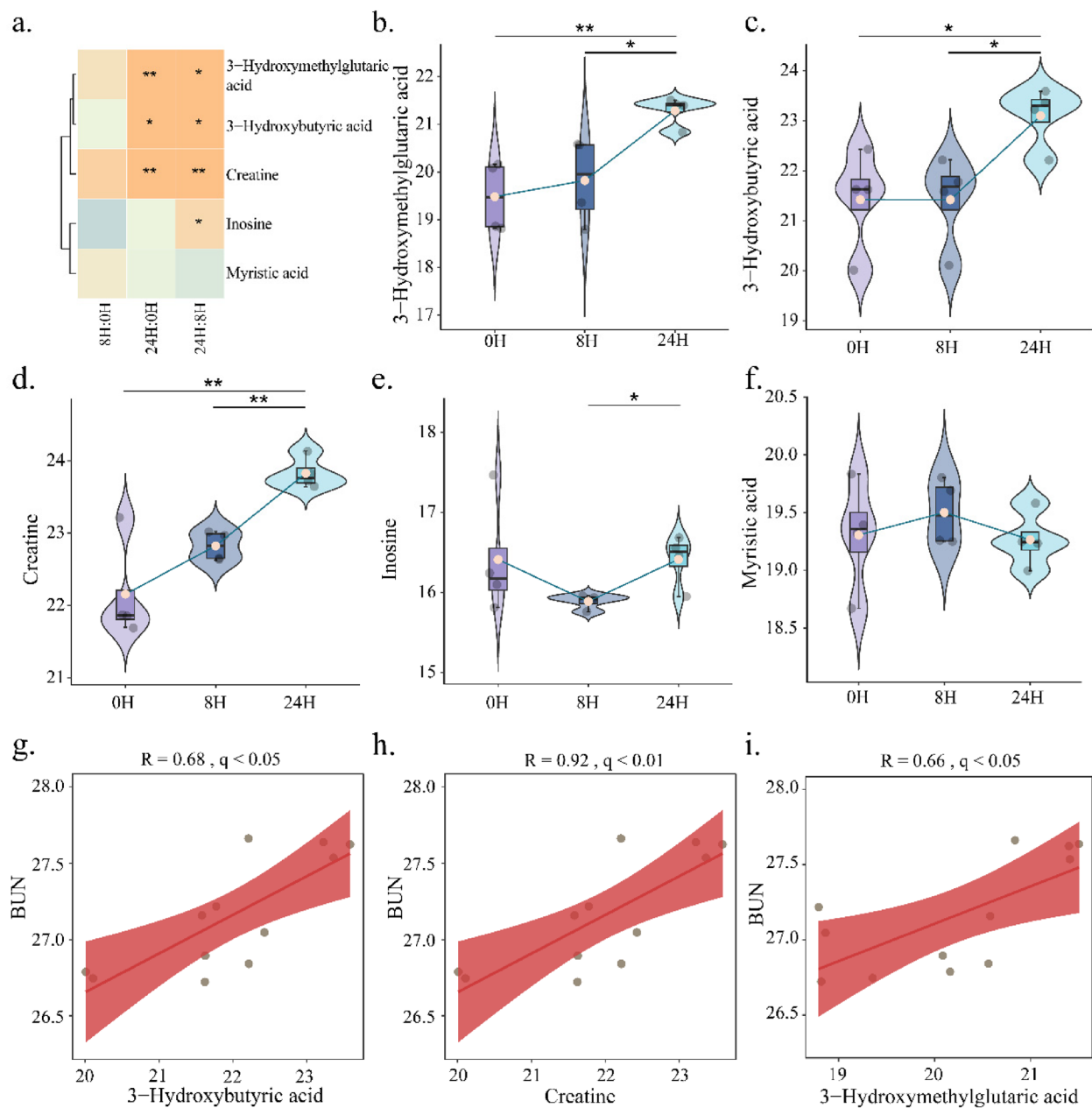


Fig. 5 Time series observation of serum metabolites in SA-AKI mice. Changes in serum metabolites in SA-AKI mice at different time points (0H, 8H, and 24H) (a–f). a, b, c, d, e, and f show the time variation of serum 3-hydroxymethylglutaric acid, 3-hydroxybutyric acid, creatine, inosine, and myristic acid, respectively. g–i Scatter plots illustrating the correlation between 3-hydroxybutyric acid, creatine, and BUN. *, $p < 0.05$; **, $p < 0.01$

to 8 h, while it showed an increasing change from 8 to 24 h ($p < 0.05$) (Fig. 5e). Myristic acid showed an increasing trend at 0 to 8 h and a decreasing trend at 8 to 24 h (Fig. 5f).

We further explored the dynamic tendency between serum core metabolites and blood urea nitrogen (BUN).

3-Hydroxybutyric acid, creatine, and 3-hydroxymethylglutaric acid demonstrated a positive correlation with BUN (3-hydroxybutyric acid: $R = 0.68, q < 0.05$; creatine: $R = 0.92, q < 0.01$; 3-hydroxymethylglutaric acid: $R = 0.66, q < 0.05$) (Fig. 5g–i). Furthermore, no significant correlations were found between inosine, myristic acid, and BUN (Additional file 4: Fig. S1a–b).

Construction of IC3 model via targeted quantitative serum metabolomics

A clinical study involving 56 patients (28 patients with sepsis vs. 28 patients with SA-AKI) was conducted to verify the diagnostic efficacy of the IC3 model with a balanced gender ratio (30 were male and 26 were female). The 30 male patients consist of 16 patients with SA-AKI and 14 patients with sepsis. For the female patients, 12 patients with SA-AKI and 14 patients with sepsis are included (Table 2). We found patients with SA-AKI showed increased levels of creatinine, urea, total and direct bilirubin, along with higher SOFA and APACHE II scores ($p < 0.05$). They also had significantly lower diastolic blood pressure and reduced platelet counts ($p < 0.05$) (Table 2).

Three core metabolites were completely detected among the 56 patients by the targeted quantitative metabolomics (Additional file 4: Table S2). The metabolite level of 3-hydroxybutyric acid ($\text{Log}_2(\text{FC}) = 3.25$, $p < 0.05$) and creatine ($\text{Log}_2(\text{FC}) = 0.33$, $p < 0.05$) were increased, while the level of inosine was decreased in SA-AKI ($\text{Log}_2(\text{FC}) = -4.06$, $p < 0.05$) (Fig. 6a). In the male patient group, 3-hydroxybutyric acid ($\text{Log}_2(\text{FC}) = 3.19$, $p < 0.01$) and creatine were significantly increased ($\text{Log}_2(\text{FC}) = 0.68$, $p < 0.01$) while inosine was significantly decreased ($\text{Log}_2(\text{FC}) = -4.64$, $p < 0.05$) in patients with SA-AKI (Additional file 4: Fig. S1c–f). In the female patient group, 3-hydroxybutyric acid was significantly increased ($\text{Log}_2(\text{FC}) = 8.77$, $p < 0.001$) while inosine was significantly decreased ($\text{Log}_2(\text{FC}) = 0.57$, $p < 0.05$), but no

Table 2 Baseline characteristics of sepsis and SA-AKI patients

	Sepsis group (n = 28)	SA-AKI group (n = 28)	P value
Age	54 ± 16	50 ± 14	0.388
Sex			0.592
Male	14 (50.0%)	16 (57.1%)	
Female	14 (50.0%)	12 (42.9%)	
HR (bpm), median, (IQR)	121 (95, 133)	105 (95, 121)	0.475
SBP (mmHg), median, (IQR)	122 (104, 153)	101 (81, 132)	0.054
DBP (mmHg), median, (IQR)	70 (60, 86)	56 (49, 67)	0.011
MAP (mmHg), median, (IQR)	88 (75, 106)	69 (61, 89)	0.029
RR (bpm), median, (IQR)	22 (17, 35)	23 (18, 28)	0.407
Temperature (°C), median, (IQR)	36.50 (36.50, 36.53)	37.05 (36.50, 38.20)	0.012
SOFA, median, (IQR)	7.00 (6.00, 8.00)	9.00 (8.75, 10.00)	< 0.001
APACHE II, median, (IQR)	15.0 (14.0, 16.0)	22.0 (20.0, 24.0)	< 0.001
WBC ($10^9/l$), median, (IQR)	15 (10, 29)	13 (9, 17)	0.210
Neutrophil ($10^9/l$), median, (IQR)	14 (9, 28)	12 (7, 15)	0.321
Monocyte ($10^9/l$), median, (IQR)	0.33 (0.21, 0.49)	0.30 (0.16, 0.36)	0.426
Lymphocyte ($10^9/l$), median, (IQR)	1.12 (0.88, 1.62)	0.79 (0.57, 0.99)	0.012
Platelet ($10^9/l$), mean ± SD	261 ± 89	152 ± 123	< 0.001
PH, median, (IQR)	7.26 (7.22, 7.43)	7.36 (7.28, 7.47)	0.059
HCO ₃ ⁻ (mmol/L), mean ± SD	20 ± 7	18 ± 6	0.161
Glucose (mmol/L), median, (IQR)	8 (7, 12)	8 (6, 9)	0.192
Lac (mmol/L), median, (IQR)	3.10 (1.80, 5.35)	2.90 (1.30, 4.80)	0.545
PCT (ng/mL), median, (IQR)	22 (2, 36)	33 (24, 46)	0.083
ALT (U/L), median, (IQR)	17 (11, 55)	17 (11, 73)	> 0.999
AST (U/L), median, (IQR)	32 (24, 87)	33 (27, 85)	0.928
Creatinine (μmol/L), median, (IQR)	117 (65, 182)	263 (158, 476)	< 0.001
Urea (mg/dl), median, (IQR)	9 (5, 15)	26 (16, 31)	< 0.001
TBIL (μmol/L), median, (IQR)	17 (7, 23)	40 (22, 84)	< 0.001
DBIL (μmol/L), median, (IQR)	7 (5, 12)	34 (13, 55)	< 0.001
IBIL (μmol/L), median, (IQR)	6 (2, 10)	11 (7, 16)	0.008

HR heart rate, BPM beats per minute, SBP systolic blood pressure, DBP diastolic blood pressure, MAP mean arterial pressure, RR respiration rate, SOFA Sequential Organ Failure Assessment, APACHE II Acute Physiological and Chronic Health Assessment, Lac lactic acid, PCT procalcitonin, ALT alanine aminotransferase, AST aspartate aminotransferase, TBIL total bilirubin, DBIL direct bilirubin, IBIL indirect bilirubin

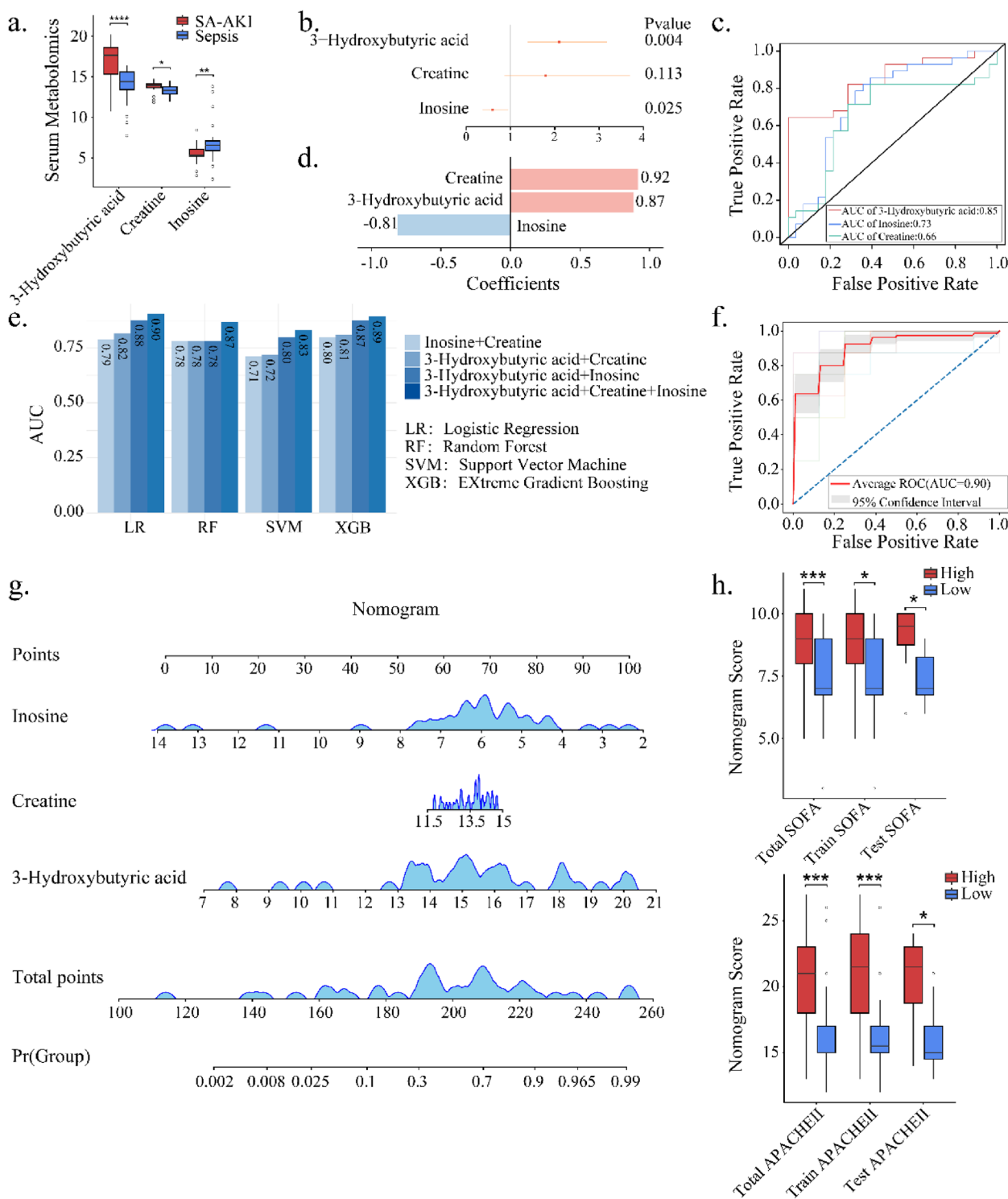


Fig. 6 Construction and Validation of the IC3 Model. **a** Abundance distribution of serum metabolites between the SA-AKI ($N=28$) group and the sepsis group ($N=28$). (Significant after Wilcoxon univariate testing ($p < 0.05$)). **b** Forest plot showing univariate logistic regression results of three metabolites. **c** ROC curves illustrating the three serum metabolites in diagnosing patients with SA-AKI. **d** Weights of the three serum metabolites in the LR model. **e** The average AUC values for different combinations of three serum metabolites in the diagnosis of SA-AKI via four machine learning methods. **f** Average AUC curve of IC3 model using the three core metabolites. **g** IC3 nomogram. **h** Distributions of SOFA and APACHE II scores for the high-risk (red) and low-risk (blue) patients, which were stratified by the median of the IC3 score. The distributions of the total sample, training set, and test set were separately shown. (Significant after two-tailed t -testing ($p < 0.05$)). *, **, and *** indicate $p < 0.05$, $p < 0.01$, and $p < 0.001$, respectively

significant change was observed for creatine in patients with SA-AKI (Additional file 4: Fig. S1c, Fig. S1g–i). To evaluate the effect of three core metabolites on SA-AKI, odds ratio (OR) was 2.10 for 3-hydroxybutyric acid ($p < 0.05$), 1.79 for creatine ($p > 0.05$), and 0.59 for inosine ($p < 0.05$) (Fig. 6b). 3-Hydroxybutyric acid demonstrated higher diagnostic accuracy for SA-AKI (AUC=0.85) in comparison to inosine (AUC=0.73) and creatine (AUC=0.66) (Fig. 6c).

When integrating the three metabolites using the logistic regression (LR) model, it exhibits a much higher predictive performance (AUC=0.90) (Fig. 6e–f). The average coefficients for 3-hydroxybutyric acid, creatine, and inosine were 0.87, 0.92, and -0.81, respectively (Fig. 6d). Moreover, an IC3 nomogram was created for a detailed assessment of each sample (Fig. 6g). Samples were categorized into high or low score groups based on the median score. SOFA and APACHE II scores were significantly higher in the high-risk group compared to the low-risk group ($p < 0.05$) (Fig. 6h), demonstrating that IC3 is also an indicator for disease severity.

Discussion

By integrating renal metabolomics and proteomics, we constructed a multi-omics molecular network of SA-AKI and identified five core metabolites associated with SA-AKI, i.e., 3-hydroxybutyric acid, creatine, inosine,

3-hydroxymethylglutaric acid and myristic acid. Subsequently, we performed a time series analysis of serum from SA-AKI mice to assess the potential of core metabolites as biomarkers for the early diagnosis of SA-AKI. Eventually, we conducted a SA-AKI diagnostic model, IC3, using serum-targeted quantitative metabolomics for SA-AKI patients with an AUC of 0.90. The major molecules associated with SA-AKI are summarized in Fig. 7.

This study employed several cutting-edge technologies, including GC-TOF-MS, 4D label-free analysis, and real-time glomerular filtration rate (GFR) monitoring technology, to enable the high-dimension and in-depth investigation of SA-AKI. 3-Hydroxybutyric acid, inosine, and creatine were identified as three core metabolites in the early stage of SA-AKI. Previous studies have shown that 3-hydroxybutyric acid is one of the ketone bodies synthesized by the liver during fasting [37, 38]. In patients with sepsis or trauma, an increase in 3-hydroxybutyric acid levels was observed [39–41], suggesting that these patients may have entered a state of ketosis due to insufficient glucose supply in the blood. In addition, the activity of inosine is highly consistent with GFR, the same conclusion was also found in previous studies [42, 43]. For instance, Szabó et al. observed that additional inosine supplementation can reduce creatinine and BUN in cecal ligation and puncture (CLP) mice [44], which potentially ameliorates acute inflammation through modulation of

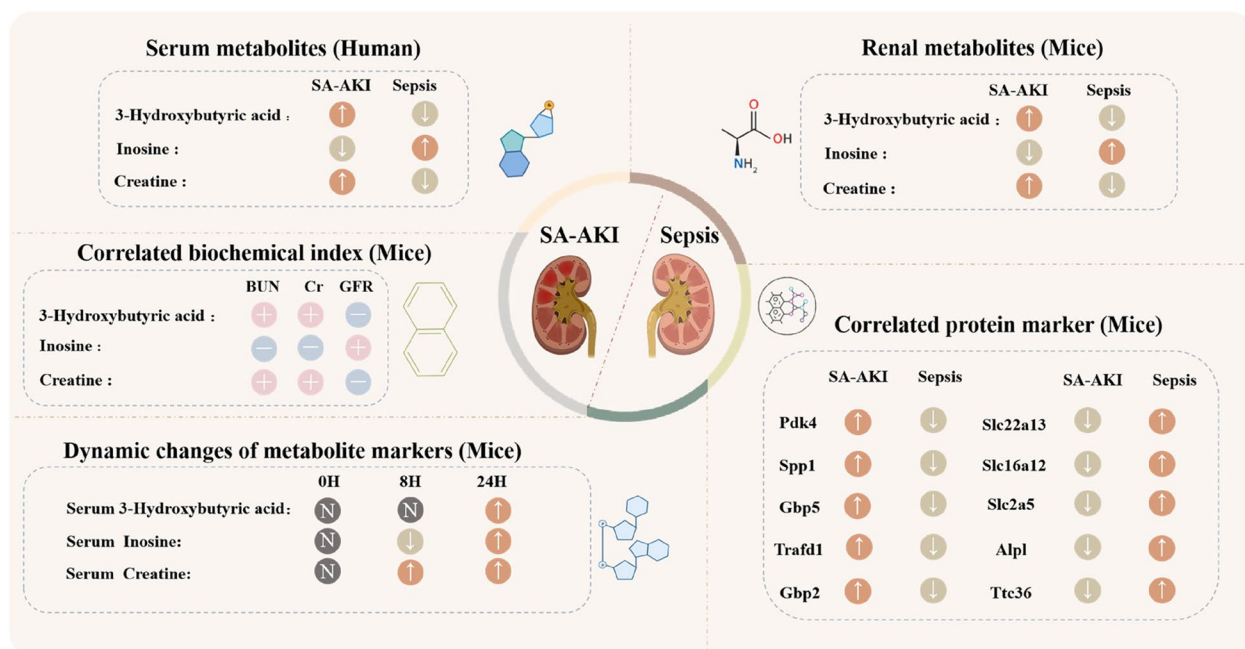


Fig. 7 Characterization of core metabolites at multiple omics levels. The main molecular changes of mice renal metabolomics, mice renal proteomics, mice plasma metabolomics, mice biochemical indicators, and clinical plasma targeted metabolomics were summarized. Arrows represent up- or down-regulation of molecules in the SA-AKI group in comparison to the sepsis group. “±” symbol indicates a positive or negative correlation between the core metabolite changes and biochemical indicators

the TLR4/NF-KB signaling pathway [45]. Furthermore, urinary creatine levels elevated in several AKI mice models induced by multiple drugs, such as polymyxin B [46], aristolochic acid [47], and gentamicin [48], which may be due to oxidative modification of renal mitochondria or cellular lysosomal creatine kinase [49, 50]. We observed that creatine continued to rise during the progression of SA-AKI, and this change affects several metabolic pathways, such as arginine and proline metabolism. Although creatine changes were not significant in female patients, creatine has the potential to be a valuable biomarker for renal injury. Drawing upon the possible significance of inosine, creatine, and 3-hydroxybutyric acid, this study formulated the IC3 model to early prediction of SA-AKI in patients with sepsis.

These three metabolites in the IC3 model have been separately used in clinic. For example, creatine is a sports supplement used to increase muscle strength, but some studies have reported that taking creatine may cause interstitial nephritis [51]. In addition, inosine supplementation effectively elevates human serum uric acid levels without compromising renal function [52–54]. However, these three core metabolites have not yet been utilized in the early screening and diagnosis of SA-AKI. We noted that early detection of 3-hydroxybutyric acid, creatine, and inosine in patients with sepsis can predict the occurrence of SA-AKI, and further found that the nomogram constructed via the IC3 model was positively correlated with APACHE II and SOFA scores. IC3 model is instrumental in the early identification of high-risk individuals among patients with sepsis who are potentially susceptible to developing SA-AKI, which can also serve as a guiding tool to assist medical care providers in offering early intervention [55]. Moreover, for SA-AKI patients with higher IC3 scores, early initiation of treatment such as renal replacement therapy (RRT) can be considered to avoid persistent renal damage and reduce mortality [56, 57].

Current researches on SA-AKI lack temporal sensitivity [57]. To this end, we performed a time series analysis of metabolites to determine the optimal time point for diagnosing SA-AKI. Because of the delay between increased creatinine concentration and the occurrence of AKI, interventions for AKI typically are initiated during the maintenance phase of renal injury [58]. Early screening for SA-AKI can be conducted within the first 24 h to promptly identify high-risk individuals, mitigate nephrotoxic drug use, and adjust dosages according to renal function; Simultaneous injecting vasoactive drugs to maintain mean arterial pressure at least 65 mmHg [59] to prevent irreversible structural renal damage. Moreover, in contrast to mice metabolomics or proteomics studies [13, 14], our work innovatively integrated three

different omics including mice renal metabolomics, renal proteomics, serum time series metabolomics, and population-targeted quantitative metabolomics to identify SA-AKI biomarkers. This multidimensional strategy greatly enhances the precision with identified biomarkers and allows us to track the dynamic change of these metabolites during the development of SA-AKI.

LPS (*i.p.*) is a classic sepsis mice model [60, 61]. Inflammatory pathways are activated, accompanied by increased mitochondrial dysfunction and disrupted energy metabolism, which further triggers metabolic reprogramming and programmed cell death in target organs, such as renal [62, 63]. This series of pathophysiological processes eventually led to the occurrence of AKI. Peng et al. found that SAP130 protein released after iron death activation can induce macrophage polarization, which further exacerbates the damage of the renal tubular [64]. On the other hand, previous studies used to apply serum creatinine, urea nitrogen, and renal pathologic score to determine whether sepsis mice were complicated with AKI [65–67]. On top of that, we combined GFR technology to successfully construct an early and stable LPS-induced SA-AKI model and double-verified it by molecular markers such as NGAL [23]. Therefore, we continued to use this technique to ensure the stability and reliability of the SA-AKI mice model.

Study limitations include the small clinical sample size and the single-center nature of participant recruitment, the potential confounders in the construction of IC3, such as medication usage, dietary habits, and lifestyle factors, only male mice were used in the experiments, and the lack of molecular mechanisms underlying these metabolic variations. Consistent with previous studies that utilized male mice [68, 69], these animals exhibit minimal individual variation and greater stability across body size, metabolic rate, and behavioral physiological responses. On the other hand, female mice experience fluctuations in estrogens and other hormones [70], which have the potential to interfere with metabolic processes and consequently influence the experimental data interpretability. Although only 56 samples were used in this study for model construction, we demonstrated the reliability of our model with multiple experimental designs, including reliable SA-AKI mice models, multi-omics of renal tissue, and serum time series metabolomics. On top of that, we are planning to expand the collection of more diverse clinical samples and conduct multi-center studies to keep updating the current model.

Conclusions

Through renal multi-omics network analyses and serum time series studies in SA-AKI mice, core metabolites were identified as potential SA-AKI diagnostic

biomarkers. Serum quantitative metabolomic analysis of a clinical cohort was performed to develop a metabolite-based diagnostic model, IC3, enabling the early detection of SA-AKI. The current results are only preliminary findings, and prospective validation in a more diverse clinical population is needed to verify the accuracy and reliability of the IC3 model.

Abbreviations

SA-AKI	Sepsis-associated acute renal injury
ICU	Intensive care unit
NGAL	Neutrophil gelatinase-associated lipocalin
KIM-1	Kidney injury molecule-1
STM	Soluble thrombomodulin
L-FABP	Liver-type fatty acid binding protein
TIMP-2	Tissue inhibitor of metalloproteinases-2
IGFBP-7	Insulin-like growth factor-binding protein 7
GFR	Glomerular filtration rate
BUN	Blood urea nitrogen
Cr	Creatinine
KDIGO	Kidney Disease Improving Global Outcomes
FDR	False discovery rate
FC	Fold change
OR	Odds ratio
ROC	Receiver operating characteristic
LR	Logistic regression
RF	Random forest
SVM	Support vector machine
XGB	Extreme gradient boosting
CLP	Cecal ligation and puncture
RRT	Renal replacement therapy

Supplementary Information

The online version contains supplementary material available at <https://doi.org/10.1186/s12916-025-03920-7>.

Additional file 1. Detailed metabolomics, proteomics sequencing methods and data quality control methods.

Additional file 2. Biochemical index and renal metabolomics data in mice. Table S1. Biochemical index between SA-AKI mice and sepsis mice. Table S2. Renal metabolomics data. Table S3. Renal metabolomics annotation.

Additional file 3. Renal proteomics analysis. Table S1. Differential renal proteins between SA-AKI and sepsis in mice. Figure S1. Mice renal proteins and enrichment analysis. a) Abundance distributions of mice renal metabolomics and proteomics. b) Heatmap showing the correlation between renal proteins and the three biochemical indicators. Orange indicates a positive correlation and blue indicates a negative correlation. c-e) Gene Ontology Enrichment Analysis for renal differential proteins, including biological process (BP) (c); cell composition (CC) (d); molecular functional (MF) (e).

Additional file 4. The expression of five core metabolites in serum metabolomics. Table S1. Serum metabolomics in SA-AKI mice. Table S2. Quantitative serum metabolomics in patients with SA-AKI or sepsis. Figure S1. Distribution of 3-Hydroxybutyric acid, inosine and creatine in male and female patients. a-b) Scatter plots illustrating the correlation between inosine, myristic acid and BUN. c) Heatmap of 3-hydroxybutyric acid, creatine, and inosine between sepsis and SA-AKI after grouping by sex. d-f) Box plot of 3-hydroxybutyric acid, inosine and creatine between sepsis and SA-AKI in male group. g-i) Box plot of 3-hydroxybutyric acid, inosine and creatine between sepsis and SA-AKI in female group. Green represents sepsis and purple represents SA-AKI. *, ** and *** indicate $p < 0.05$, $p < 0.01$, and $p < 0.001$, respectively. Renal proteomics data has been deposited in the ProteomeXchange Consortium via the PRIDE (Proteomics Identifications) partner repository with the dataset identifier PXD057050.

Acknowledgements

We thank all the workers who contributed to this study.

Authors' contributions

L.C., C.W., K.Y.: Conceptualization, data analysis, writing - original draft, writing - review & editing, funding acquisition; M.Z.: Conceptualization, data analysis, writing - original draft, writing - review & editing; P.H., Y.L.1: Data analysis, writing - original draft, writing - review & editing; Y.L.2, Y.X.1: Provide material; C.N.: Data analysis, funding acquisition; Y.L.3, Y.F., N.J., Y.P., D.W., Y.Z.1.: Visualization; F.L., X.W.1, X.W.2, H.L.: Acquisition; Y.Z.2, W.Z., Y.L.4: Validation; M.Y., Y.Z.3, Y.S., Y.X.2, L.S.: Data curation and interpretation; All authors read and approved the final manuscript.

Funding

This project was funded by the National Natural Science Foundation of China-Regional Innovation and Development Joint Fund (U20A20366), the National Natural Science Foundation of China (32370711), the Natural Science Foundation of Heilongjiang Province (JQ2021H003), Shenzhen science and technology research and development fund (JCYJ20210324114000001, JCYJ20220530152409020), and Shenzhen Medical Research Fund (A2303033). Declaration.

Declarations

Ethics approval and consent to participate

Mice experiments were approved by the Laboratory Animal Management and Welfare Ethics Committee of the First Affiliated Hospital of Harbin Medical University (Ethical Approval Number:2023022). The clinical investigation was approved by the Ethics Committee of the Second Affiliated Hospital of Harbin Medical University (Ethical Approval Number: KY2021-188) and strictly complied with the ethical standards of the Declaration of Helsinki. In this study, all research was conducted in accordance with the Declaration of Helsinki. Written informed consent was duly obtained from all patients.

Consent for publication

Not applicable.

Competing interests

The authors declare no competing interests.

Author details

¹Department of Critical Care Medicine, The First Affiliated Hospital of Harbin Medical University, Harbin, Heilongjiang 150001, China. ²Department of Critical Care Medicine, First Affiliated Hospital of Southern, Shenzhen People's Hospital, University of Science and Technology, Shenzhen 518020, China. ³Department of Critical Care Medicine, Second Affiliated Hospital of Harbin Medical University, Harbin, Heilongjiang Province 150086, China. ⁴Department of Critical Care Medicine, Harbin Medical University Cancer Hospital, Harbin 150081, China. ⁵Heilongjiang Provincial Key Laboratory of Critical Care Medicine, 23 Postal Street, Nangang District, Harbin, Heilongjiang 150001, China.

Received: 11 August 2024 Accepted: 30 January 2025

Published online: 11 February 2025

References

- Kempker JA, Martin GS. A global accounting of sepsis. *Lancet*. 2020;395(10219):168–70.
- Singer M, Deutschman CS, Seymour CW, Shankar-Hari M, Annane D, Bauer M, et al. The third international consensus definitions for sepsis and septic shock (Sepsis-3). *JAMA*. 2016;315(8):801–10.
- Murugan R, Karajala-Subramanyam V, Lee M, Yende S, Kong L, Carter M, et al. Acute kidney injury in non-severe pneumonia is associated with an increased immune response and lower survival. *Kidney Int*. 2010;77(6):527–35.
- Vincent JL, Sakr Y, Sprung CL, Ranieri VM, Reinhart K, Gerlach H, et al. Sepsis in European intensive care units: results of the SOAP study. *Crit Care Med*. 2006;34(2):344–53.

5. Chertow GM, Burdick E, Honour M, Bonventre JV, Bates DW. Acute kidney injury, mortality, length of stay, and costs in hospitalized patients. *J Am Soc Nephrol*. 2005;16(11):3365–70.
6. Bellomo R, Kellum JA, Ronco C, Wald R, Martensson J, Maiden M, et al. Acute kidney injury in sepsis. *Intensive Care Med*. 2017;43(6):816–28.
7. Nickolas TL, Schmidt-Ott KM, Canetta P, Forster C, Singer E, Sise M, et al. Diagnostic and prognostic stratification in the emergency department using urinary biomarkers of nephron damage: a multicenter prospective cohort study. *J Am Coll Cardiol*. 2012;59(3):246–55.
8. Srisawat N, Murugan R, Lee M, Kong L, Carter M, Angus DC, et al. Plasma neutrophil gelatinase-associated lipocalin predicts recovery from acute kidney injury following community-acquired pneumonia. *Kidney Int*. 2011;80(5):545–52.
9. Wheeler DS, Devarajan P, Ma Q, Harmon K, Monaco M, Cvijanovich N, et al. Serum neutrophil gelatinase-associated lipocalin (NGAL) as a marker of acute kidney injury in critically ill children with septic shock. *Crit Care Med*. 2008;36(4):1297–303.
10. Bell M, Larsson A, Venge P, Bellomo R, Mårtensson J. Assessment of cell-cycle arrest biomarkers to predict early and delayed acute kidney injury. *Dis Markers*. 2015;2015: 158658.
11. Tu Y, Wang H, Sun R, Ni Y, Ma L, Xv F, et al. Urinary netrin-1 and KIM-1 as early biomarkers for septic acute kidney injury. *Ren Fail*. 2014;36(10):1559–63.
12. Kalim S, Rhee EP. An overview of renal metabolomics. *Kidney Int*. 2017;91(1):61–9.
13. Hato T, Zollman A, Plotkin Z, El-Achkar TM, Maier BF, Pay SL, et al. Endotoxin preconditioning reprograms S1 tubules and macrophages to protect the kidney. *J Am Soc Nephrol*. 2018;29(1):104–17.
14. Xu J, Li J, Li Y, Shi X, Zhu H, Chen L. Multidimensional landscape of SA-AKI revealed by integrated proteomics and metabolomics analysis. *Biomolecules*. 2023;13(9):1329.
15. Gisewhite S, Stewart IJ, Beilman G, Luszczek E. Urinary metabolites predict mortality or need for renal replacement therapy after combat injury. *Crit Care*. 2021;25(1):119.
16. Wang Z, Xu J, Zhang Y, Chen C, Kong C, Tang L, et al. Prediction of acute kidney injury incidence following acute type A aortic dissection surgery with novel biomarkers: a prospective observational study. *BMC Med*. 2023;21(1):503.
17. Jin N, Nan C, Li W, Lin P, Xin Y, Wang J, et al. PAGE-based transfer learning from single-cell to bulk sequencing enhances model generalization for sepsis diagnosis. *Brief Bioinform*. 2024;26(1):bbae661.
18. Schreiber A, Shulhevich Y, Geraci S, Hesser J, Stsepankou D, Neudecker S, et al. Transcutaneous measurement of renal function in conscious mice. *Am J Physiol Renal Physiol*. 2012;303(5):F783–8.
19. Schock-Kusch D, Sadick M, Henninger N, Kraenzlin B, Claus G, Kloetzer HM, et al. Transcutaneous measurement of glomerular filtration rate using FITC-sinistrin in rats. *Nephrol Dial Transplant*. 2009;24(10):2997–3001.
20. Seymour CW, Liu VX, Iwashyna TJ, Brunkhorst FM, Rea TD, Scherag A, et al. Assessment of clinical criteria for sepsis: for the third international consensus definitions for sepsis and septic shock (Sepsis-3). *JAMA*. 2016;315(8):762–74.
21. Summary of Recommendation Statements. *Kidney Int Suppl* (2011). 2012;2(1):8–12. <https://doi.org/10.1038/kisup.2012.7>.
22. Thomas ME, Blaine C, Dawnay A, Devonald MA, Ftouh S, Laing C, et al. The definition of acute kidney injury and its use in practice. *Kidney Int*. 2015;87(1):62–73.
23. Xin Y, Liu Y, Liu L, Wang X, Wang D, Song Y, et al. Dynamic changes in the real-time glomerular filtration rate and kidney injury markers in different acute kidney injury models. *J Transl Med*. 2024;22(1):857.
24. Tsugawa H, Tsujimoto Y, Arita M, Bamba T, Fukusaki E. GC/MS based metabolomics: development of a data mining system for metabolite identification by using soft independent modeling of class analogy (SIMCA). *BMC Bioinformatics*. 2011;12: 131.
25. Kind T, Wohlgemuth G, Lee DY, Lu Y, Palazoglu M, Shahbaz S, et al. FiehnLib: mass spectral and retention index libraries for metabolomics based on quadrupole and time-of-flight gas chromatography/mass spectrometry. *Anal Chem*. 2009;81(24):10038–48.
26. Matyash V, Liebisch G, Kurzchalia TV, Shevchenko A, Schwudke D. Lipid extraction by methyl-tert-butyl ether for high-throughput lipidomics. *J Lipid Res*. 2008;49(5):1137–46.
27. Xuan Q, Hu C, Yu D, Wang L, Zhou Y, Zhao X, et al. Development of a high coverage pseudotargeted lipidomics method based on ultra-high performance liquid chromatography-mass spectrometry. *Anal Chem*. 2018;90(12):7608–16.
28. Chen W, Gong L, Guo Z, Wang W, Zhang H, Liu X, et al. A novel integrated method for large-scale detection, identification, and quantification of widely targeted metabolites: application in the study of rice metabolomics. *Mol Plant*. 2013;6(6):1769–80.
29. An Z, Hu T, Lv Y, Li P, Liu L. Targeted amino acid and related amines analysis based on iTRAQ[®]-LC-MS/MS for discovering potential hepatotoxicity biomarkers. *J Pharm Biomed Anal*. 2020;178: 112812.
30. Du Y, Cai T, Li T, Xue P, Zhou B, He X, et al. Lysine malonylation is elevated in type 2 diabetic mouse models and enriched in metabolic associated proteins. *Mol Cell Proteomics*. 2015;14(1):227–36.
31. Zeng X, Zhou X, Zhou J, Zhou H, Hong X, Li D, et al. Limonin mitigates cisplatin-induced acute kidney injury through metabolic reprogramming. *Biomed Pharmacother*. 2023;167: 115531.
32. Meng H, Sengupta A, Ricciotti E, Mrčela A, Mathew D, Mazaleuskaya LL, et al. Deep phenotyping of the lipidomic response in COVID-19 and non-COVID-19 sepsis. *Clin Transl Med*. 2023;13(11): e1440.
33. Ibáñez-Prada ED, Guerrero JL, Bustos IG, León L, Fuentes YV, Santamaría-Torres M, et al. The unique metabolic and lipid profiles of patients with severe COVID-19 compared to severe community-acquired pneumonia: a potential prognostic and therapeutic target. *Expert Rev Respir Med*. 2024;18(10):815–29.
34. Standage SW, Xu S, Brown L, Ma Q, Koterba A, Lahni P, et al. NMR-based serum and urine metabolomic profile reveals suppression of mitochondrial pathways in experimental sepsis-associated acute kidney injury. *Am J Physiol Renal Physiol*. 2021;320(5):F984-f1000.
35. Feng Q, Yang Y, Ren K, Qiao Y, Sun Z, Pan S, et al. Broadening horizons: the multifaceted functions of ferroptosis in kidney diseases. *Int J Biol Sci*. 2023;19(12):3726–43.
36. Zhang X, Wu W, Li Y, Peng Z. Exploring the role and therapeutic potential of lipid metabolism in acute kidney injury. *Ren Fail*. 2024;46(2): 2403652.
37. Møller N. Ketone body, 3-hydroxybutyrate: minor metabolite - Major medical manifestations. *J Clin Endocrinol Metab*. 2020;105(9):2884.
38. Hsu TT, Leiske DL, Rosenfeld L, Sonner JM, Fuller GG. 3-Hydroxybutyric acid interacts with lipid monolayers at concentrations that impair consciousness. *Langmuir*. 2013;29(6):1948–55.
39. Pandey S, Siddiqui MA, Azim A, Sinha N. Metabolic fingerprint of patients showing responsiveness to treatment of septic shock in intensive care unit. *MAGMA*. 2023;36(4):659–69.
40. Park G, Munley JA, Kelly LS, Kannan KB, Mankowski RT, Sharma A, et al. Gut microbiome dysbiosis after sepsis and trauma. *Crit Care*. 2024;28(1):18.
41. Mickiewicz B, Tam P, Jenne CN, Leger C, Wong J, Winston BW, et al. Integration of metabolic and inflammatory mediator profiles as a potential prognostic approach for septic shock in the intensive care unit. *Crit Care*. 2015;19(1):11.
42. Garcia Soriano F, Liaudet L, Marton A, Haskó G, Batista Lorigados C, Deitch EA, et al. Inosine improves gut permeability and vascular reactivity in endotoxic shock. *Crit Care Med*. 2001;29(4):703–8.
43. Chen H, Chen JB, Du LN, Yuan HX, Shan JJ, Wang SC, et al. Integration of lipidomics and metabolomics reveals plasma and urinary profiles associated with pediatric *Mycoplasma pneumoniae* infections and its severity. *Biomed Chromatogr*. 2024;38(4): e5817.
44. Liaudet L, Mabley JG, Soriano FG, Pacher P, Marton A, Haskó G, et al. Inosine reduces systemic inflammation and improves survival in septic shock induced by cecal ligation and puncture. *Am J Respir Crit Care Med*. 2001;164(7):1213–20.
45. Mao B, Guo W, Tang X, Zhang Q, Yang B, Zhao J, et al. Inosine pretreatment attenuates LPS-induced lung injury through regulating the TLR4/MyD88/NF- κ B signaling pathway in vivo. *Nutrients*. 2022;14(14):2830.
46. Jeong ES, Kim G, Moon KS, Kim YB, Oh JH, Kim HS, et al. Characterization of urinary metabolites as biomarkers of colistin-induced nephrotoxicity in rats by a liquid chromatography/mass spectrometry-based metabolomics approach. *Toxicol Lett*. 2016;248:52–60.
47. Sieber M, Hoffmann D, Adler M, Vaidya VS, Clement M, Bonventre JV, et al. Comparative analysis of novel noninvasive renal biomarkers and metabolomic changes in a rat model of gentamicin nephrotoxicity. *Toxicol Sci*. 2009;109(2):336–49.

48. Zhao YY, Tang DD, Chen H, Mao JR, Bai X, Cheng XH, et al. Urinary metabolomics and biomarkers of aristolochic acid nephrotoxicity by UPLC-QTOF/HDMS. *Bioanalysis*. 2015;7(6):685–700.
49. Schlattner U, Tokarska-Schlattner M, Wallimann T. Mitochondrial creatine kinase in human health and disease. *Biochim Biophys Acta*. 2006;1762(2):164–80.
50. Dai C, Li J, Tang S, Li J, Xiao X. Colistin-induced nephrotoxicity in mice involves the mitochondrial, death receptor, and endoplasmic reticulum pathways. *Antimicrob Agents Chemother*. 2014;58(7):4075–85.
51. Koshy KM, Griswold E, Schneeberger EE. Interstitial nephritis in a patient taking creatine. *N Engl J Med*. 1999;340(10):814–5.
52. Liang N, Wu M, Gao Y, Yang S, Lin X, Sun H, et al. Purine metabolic pathway alterations and serum urate changes after oral inosine loading in male Chinese volunteers. *Mol Nutr Food Res*. 2024;68(2): e2300115.
53. Dalbeth N, Mihov B, Stewart A, Gamble GD, Merriman TR, Mount D, et al. Effects of elevated serum urate on cardiometabolic and kidney function markers in a randomised clinical trial of inosine supplementation. *Sci Rep*. 2022;12(1):12887.
54. Dalbeth N, Horne A, Mihov B, Stewart A, Gamble GD, Merriman TR, et al. Elevated urate levels do not alter bone turnover markers: randomized controlled trial of inosine supplementation in postmenopausal women. *Arthritis Rheumatol*. 2021;73(9):1758–64.
55. Stanski NL, Rodrigues CE, Strader M, Murray PT, Endre ZH, Bagshaw SM. Precision management of acute kidney injury in the intensive care unit: current state of the art. *Intensive Care Med*. 2023;49(9):1049–61.
56. Boutin L, Latosinska A, Mischak H, Deniau B, Asakage A, Legrand M, et al. Subclinical and clinical acute kidney injury share similar urinary peptide signatures and prognosis. *Intensive Care Med*. 2023;49(10):1191–202.
57. Vanmassenhove J, Kielstein J, Jörres A, Biesen WV. Management of patients at risk of acute kidney injury. *Lancet*. 2017;389(10084):2139–51.
58. Perazella MA, Coca SG. Three feasible strategies to minimize kidney injury in “incipient AKI.” *Nat Rev Nephrol*. 2013;9(8):484–90.
59. Joannidis M, Druml W, Forni LG, Groeneveld ABJ, Honore PM, Hoste E, et al. Prevention of acute kidney injury and protection of renal function in the intensive care unit: update 2017: expert opinion of the Working Group on Prevention, AKI section, European Society of Intensive Care Medicine. *Intensive Care Med*. 2017;43(6):730–49.
60. Li S, Zhang Y, Lu R, Lv X, Lei Q, Tang D, et al. Peroxiredoxin 1 aggravates acute kidney injury by promoting inflammation through Mincle/Syk/NF- κ B signaling. *Kidney Int*. 2023;104(2):305–23.
61. Böhner AMC, Jacob AM, Heuser C, Stumpf NE, Effland A, Abdullah Z, et al. Renal denervation exacerbates LPS- and antibody-induced acute kidney injury, but protects from pyelonephritis in mice. *J Am Soc Nephrol*. 2021;32(10):2445–53.
62. Soto-Herederó G, de Las Gómez, Heras MM, Gabandé-Rodríguez E, Oller J, Mittelbrunn M. Glycolysis - a key player in the inflammatory response. *Febs J*. 2020;287(16):3350–69.
63. Liu AB, Tan B, Yang P, Tian N, Li JK, Wang SC, et al. The role of inflammatory response and metabolic reprogramming in sepsis-associated acute kidney injury: mechanistic insights and therapeutic potential. *Front Immunol*. 2024;15: 1487576.
64. Zhang J, Jiang J, Wang B, Wang Y, Qian Y, Suo J, et al. SAP130 released by ferroptosis tubular epithelial cells promotes macrophage polarization via Mincle signaling in sepsis acute kidney injury. *Int Immunopharmacol*. 2024;129: 111564.
65. Ferrè S, Deng Y, Huen SC, Lu CY, Scherer PE, Igarashi P, et al. Renal tubular cell spliced X-box binding protein 1 (Xbp1s) has a unique role in sepsis-induced acute kidney injury and inflammation. *Kidney Int*. 2019;96(6):1359–73.
66. Zhang B, Zeng M, Wang Y, Li M, Wu Y, Xu R, et al. Oleic acid alleviates LPS-induced acute kidney injury by restraining inflammation and oxidative stress via the Ras/MAPKs/PPAR- γ signaling pathway. *Phytomedicine*. 2022;94: 153818.
67. Lee SH, Kim KH, Lee SM, Park SJ, Lee S, Cha RH, et al. STAT3 blockade ameliorates LPS-induced kidney injury through macrophage-driven inflammation. *Cell Commun Signal*. 2024;22(1):476.
68. Charlton JR, Xu Y, Wu T, deRonde KA, Hughes JL, Dutta S, et al. Magnetic resonance imaging accurately tracks kidney pathology and heterogeneity in the transition from acute kidney injury to chronic kidney disease. *Kidney Int*. 2021;99(1):173–85.
69. Chen J, Xu C, Yang K, Gao R, Cao Y, Liang L, et al. Inhibition of ALKBH5 attenuates I/R-induced renal injury in male mice by promoting Ccl28 m6A modification and increasing Treg recruitment. *Nat Commun*. 2023;14(1):1161.
70. Zhu L, Zou F, Yang Y, Xu P, Saito K, Othrell Hinton A, Jr., et al. Estrogens prevent metabolic dysfunctions induced by circadian disruptions in female mice. *Endocrinology*. 2015;156(6):2114–23.

Publisher's Note

Springer Nature remains neutral with regard to jurisdictional claims in published maps and institutional affiliations.